J Therm Anal Calorim (2010) 101:169–173
DOI 10.1007/s10973-009-0430-8

Thermal expansion and heat capacity of dysprosium hafnate

G. Panneerselvam · R. Venkata Krishnan · K. Nagarajan · M. P. Antony

Received: 23 July 2009 / Accepted: 17 August 2009 / Published online: 18 September 2009

Abstract Dysprosium hafnate is a candidate material for as control rods in nuclear reactor because dysprosium (Dy) and hafnium (Hf) have very high absorption cross-sections for neutrons. Dysprosium hafnate ($Dy_2O_3{\cdot}2HfO_2$-fluorite phase solid solution) was prepared by solid-state as well as wet chemical routes. The fluorite phase of the compound was characterized by using X-ray diffraction (XRD). Thermal expansion characteristics were studied using high temperature X-ray diffraction (HTXRD) in the temperature range 298–1973 K. Heat capacity measurements of dysprosium hafnate were carried out using differential scanning calorimetry (DSC) in the temperature range 298–800 K. The room temperature lattice parameter and the coefficient of thermal expansion are 0.5194 nm and 7.69×10^{-6} K^{-1}, respectively. The heat capacity value at 298 K is 232 J mol^{-1} K^{-1}.

Keywords Dysprosium hafnate · Control rod · Heat capacity · Thermal expansion · HTXRD

Introduction

Boron in the form of boron carbide, B_4C, is generally used in the control rods of fast breeder reactors. The major advantages of boron carbide are the relatively high neutron absorption cross section for boron, high thermal stability and commercial availability. However, it is less resistant to radiation damage due to the reaction $5B^{10}$ $[n,\alpha]$ $_3Li^6$ which results in helium formation. These helium bubbles nucleate cracks and thereby reduce lifetime of control rods. Cadmium, iridium, hafnium and their compounds have also been used as control rod materials [1] due to their large absorption cross-sections. Good amount of work has been carried out on other potential neuron absorber materials, which do not swell during irradiation. These include ceramic materials based on Dy, Eu, Sm, Gd [2, 3] and pure Hf and Hf alloys. Post-irradiation examination revealed that lanthanide oxides (Ln_2O_3–MO_2) have the highest resistance towards radiation damage among the ceramic absorbers [2]. Though dysprosium titanate is an attractive control rod material for the thermal nuclear reactor [4], due to its high neutron absorption cross section, relatively low swelling, no out-gassing under neutron irradiation, high melting point, non-interactive nature with the cladding at high temperatures, etc., they are sensitive to composition changes caused during synthesis which complicates its production technology. A phase formed as a result of deviations from the initial composition of the synthesized compound has lower radiation resistance [5]. Dysprosium hafnate is considered to be a better control rod material compared to dysprosium titanate because stable fluorite structure exists with HfO_2 containing 12–55 mol% Dy_2O_3 [5]. It also possesses good radiation resistance, high neutron absorption cross section, lifetime, etc., [6, 7] and unlike dysprosium titanate where only Dy is a neutron absorber, both Dy and Hf are neutron absorbers and thereby the physical efficiency of the control rod is more than that of dysprosium titanate. Heat capacities determinations of various compounds have attracted many researchers' attention [8, 9]. The only data available in the literature on the heat capacity and thermal expansion of dysprosium hafnate is from Risovany et al. [6]. The temperature range of measurement for thermal expansion is from 293 to 773 K and for heat capacity from

G. Panneerselvam · R. Venkata Krishnan · K. Nagarajan · M. P. Antony (✉)
Fuel Chemistry Division, Chemistry Group, Indira Gandhi Centre for Atomic Research, Kalpakkam 603 102, India
e-mail: mpa@igcar.gov.in

350 to 673 K. Also, the heat capacity data show large scatter in measured data. Therefore, heat capacity and thermal expansion measurements on dysprosium hafnate were carried out in the temperature range 298–800 K and 298–1973 K, respectively.

Experimental

The oxides of dysprosium and hafnium (99.9%) used in this study were obtained from M/s Indian Rare Earths, India. Dysprosium hafnate was prepared by standard solid-state synthesis (ceramic method) route as well as by wet chemical methods.

Solid-state synthesis

For solid-state synthesis, stiochiometric amounts of dysprosium and hafnium oxide powders were mixed for about 1 h in an agate mortar. The homogeneous powder mix was compacted at a pressure of 500 MPa, using a uniaxial hydraulic press to get pellets. The green pellets were initially sintered at 1,373 K for 8 h. The pellets were subsequently ground to get fine powders that were compacted again and heated at 1,773 K for another 10 h to get final sintered pellets.

Wet chemical synthesis

For wet chemical synthesis, stiochiometric amounts of dysprosium and hafnium oxides were dissolved in concentrated HNO_3. The solution was then evaporated to obtain dry powder. The powder was calcined at 1,273 K for 8 h. The sample was then ground, compacted, and sintered at 1,673 K for 8 h. The phase characterization and lattice parameter measurements were carried out by X-ray diffraction technique.

X-ray diffraction studies

For characterization by X-ray powder diffraction, the sintered pellet was powdered to obtain $\approx$100 μm-sized particles. The XRD experiment was performed using Cu Kα radiation ($\lambda = 154.098$ pm), in a Philips X'pert MPD system that is equipped with a graphite monochromator and a scintillation detector. The X-ray diffraction pattern was recorded in the two-theta range, $10 < 2\theta < 80°$. Peak positions and the relative intensities were estimated using a peak-fit program of the Philips X'pert Plus software. The calibration of the diffractometer was carried out using silicon and α-alumina standards obtained from the National Institute of Standards and Technology (NIST), USA.

Thermal expansion measurements

The thermal expansion behaviour was studied from room temperature to 1,973 K at a pressure of 10^{-6} mbar using the XRD-HDK 2.4 high temperature attachment in Philips X'pert MPD system. The detailed description of the HTXRD procedure has already been described elsewhere [10]. The temperature of the sample was controlled within ±1 K. Before each run, the vacuum chamber was first evacuated to a pressure of about 10^{-6} mbar and then filled with high pure argon gas. The evacuation and argon filling cycle was repeated four to five times, before the X-ray patterns were recorded.

Heat capacity measurements

A heat flux type differential scanning calorimeter (model number DSC821e/700 of M/s. Mettler Toledo GmbH, Switzerland) was used in this study. Pellet samples were hermetically sealed in 40 μl Al-pans. High purity argon was used as the purge gas at a flow rate of 50 ml min^{-1} and a heating rate of 10 K min^{-1} was employed in DSC measurements in the temperature range 298–800 K. A thin disc of sapphire was used as the heat capacity standard. A three segment-heating programme was used. The first segment lasting for 5 min was an isothermal one at the initial temperature, the second segment was a dynamic one with a heating rate of 10 K min^{-1}, and the final segment lasting for 5 min was another isothermal one at the final temperature. Temperature, heat and heat rate calibrations of the DSC were carried out, as explained in our earlier work [11]

Results

Thermal expansion of $Dy_2O_3 \cdot 2HfO_2$

In Fig. 1, we present the room temperature (298 K) XRD patterns of dysprosium hafnate. It was observed from the XRD patterns that the dysprosium hafnate crystallizes into cubic structure with space group Fm3m (225). The lattice parameter of dysprosium hafnate at room temperature is 0.5194 nm. The diffraction patterns and the lattice parameter values are in good agreement with the literature data [12]. The lattice parameter (a) in each case was estimated by considering the eight major reflections of the CaF_2 structure (see Fig. 1). Finally, an effective high angle corrected lattice parameter at each temperature is obtained by the standard Nelson–Riley extrapolation procedure [13]. The HTXRD studies were carried out on the samples prepared by both the preparation methods namely wet chemical and solid-state synthesis. The difference in the lattice parameter estimated from the XRD pattern at different temperatures between the

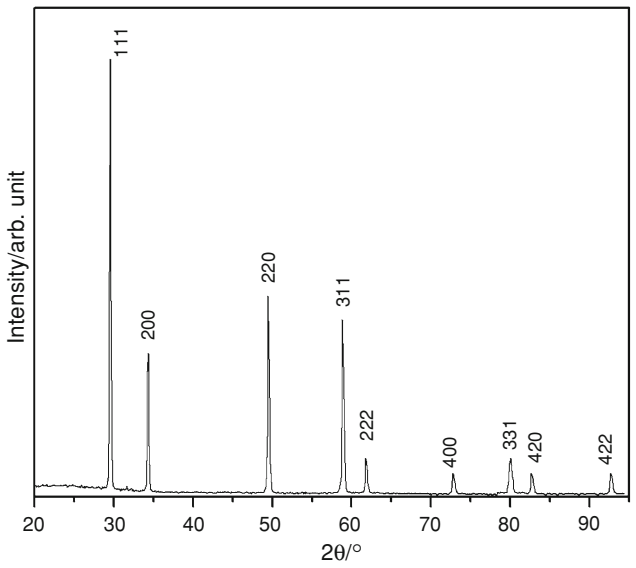

Fig. 1 Room temperature XRD pattern of $Dy_2O_3{\cdot}2HfO_2$

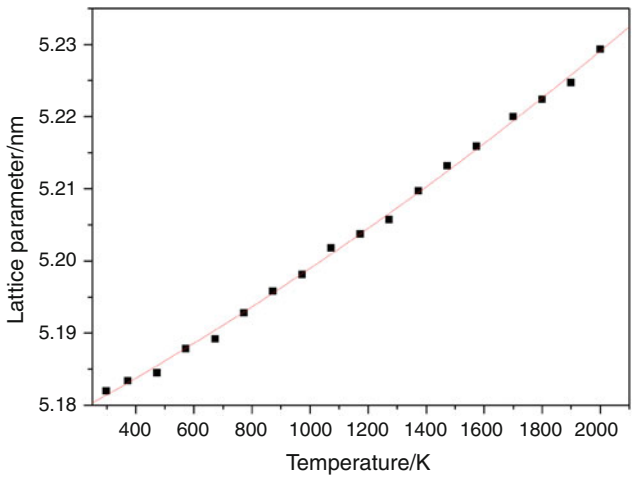

Fig. 2 Lattice expansion of $Dy_2O_3{\cdot}2HfO_2$ as a function of temperature

solid solution prepared by wet chemical and solid-state route is within ±0.0004 nm. Therefore, an average value of the computed lattice parameter is being reported. Figure 2 shows the effective lattice parameter thus obtained as a function of temperature. The lattice parameter data as a function of temperature is also listed in Table 1.

For the purpose of calculating thermal expansivities, the corrected lattice parameter data with temperature (K) are fitted to a second-degree polynomial in the temperature increment (T-298).

$$a(\text{nm}) = 0.51815 + 3.9830 \times 10^{-6}(T\text{-}298) + 9.5380 \times 10^{-10}(T\text{-}298)^2 \quad (1)$$

where T is the temperature in Kelvin. From the above relation instantaneous (α_L-instantaneous), mean (α_L-mean) and relative (α_L-relative) linear thermal expansion coefficients are computed as given below

$$\alpha_i\text{-instantaneous} = (1/a_T)(da_T/dT) \quad (2)$$

$$\alpha_m\text{-mean} = (1/a_{298}) \times \{(a_T - a_{298})/T - 298)\} \quad (3)$$

$$\alpha_r\text{-relative} = (1/a_{298})(da_T/dT) \quad (4)$$

$$\text{Expansion}\ (\%) = 100 \times \{(a_T - a_{298})/a_{298}\} \quad (5)$$

In the above expression, a_T and a_{298} represents the lattice parameter at temperature T and at 298 K, respectively. The percentage linear thermal expansion computed using Eq. 5 was fitted to a second-degree polynomial in temperature and the expression is given below and is also shown in Fig. 3.

$$\text{Expansion}(\%) = -0.2407 + 7.6685 \times 10^{-4}T + 1.8363 \times 10^{-7}T^2 \quad (6)$$

.

Table 1 The lattice parameter as a function of temperature, instantaneous (α_i), mean (α_m), relative (α_r) linear thermal expansivities

HT-XRD data of $Dy_2O_3{\cdot}2HfO_2$					
T/K	a/nm	$\alpha_i/(10^{-6}\ K^{-1})$	$\alpha_m/(10^{-6}\ K^{-1})$	$\alpha_r/(10^{-6}\ K^{-1})$	TE/%
298	0.5194	8.76	8.80	8.76	0.00
373	0.5198	9.03	9.07	9.04	0.07
473	0.5202	9.39	9.44	9.41	0.16
573	0.5207	9.75	9.80	9.77	0.26
673	0.5213	10.11	10.16	10.14	0.36
773	0.5218	10.47	10.53	10.51	0.46
873	0.5224	10.83	10.89	10.87	0.57
973	0.5229	11.18	11.25	11.24	0.68
1,073	0.5235	11.54	11.62	11.61	0.79
1,173	0.5241	11.90	11.98	11.98	0.91
1,273	0.5248	12.25	12.35	12.34	1.03
1,373	0.5254	12.60	12.71	12.71	1.16
1,473	0.5261	12.96	13.07	13.08	1.29
1,573	0.5268	13.31	13.44	13.45	1.42
1,700	0.5275	13.66	13.80	13.81	1.56
1,800	0.5282	14.02	14.16	14.18	1.70
1,900	0.5290	14.37	14.53	14.55	1.84
2,000	0.5297	14.72	14.89	14.91	1.99

Heat capacity of $Dy_2O_3{\cdot}2HfO_2$

Heat capacity data of sapphire given by National Institute of Standards and Technology, USA (NIST) were used for computing the heat capacities of the samples. Heat capacity of $Dy_2O_3{\cdot}2HfO_2$ measured by DSC and given in Table 2 are the mean of eight measurements. The difference in the

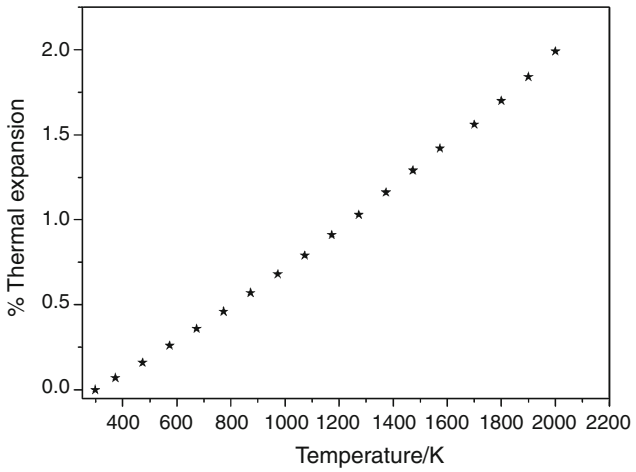

Fig. 3 Thermal expansion characteristics of $Dy_2O_3{\cdot}2HfO_2$

measured heat capacity values between the samples prepared by wet chemical and solid-state synthesis is within 1–3% which is within the standard deviation between measurements. Therefore, an average value of the measured heat capacity is reported. The uncertainty in the error in the heat capacity values by our DSC measurements had been earlier determined to be ±3% by measurements on ThO_2 samples [14]. However, the relative standard deviations among the present measurements are in the range of 1–3%. Therefore, the uncertainty in the measured heat capacity values has been estimated to be ±3%. The measured heat capacity of $Dy_2O_3{\cdot}2HfO_2$ were least squares fitted to obtain the following polynomial in temperature

$$C_{p,m}(Dy_2O_3 \cdot 2HfO_2)\left(J\,mol^{-1}\ K^{-1}\right) = 111.27 + 3.8583 \times 10^{-1}(T/K) + 2.318715 \times 10^{6}(K/T)^2 - 2.2 \times 10^{-4}(T/K)^2(298 - 800\ K) \quad (7)$$

The standard error of the fit is 1.8 J K^{-1} mol.$^{-1}$. The measured heat capacity of $Dy_2O_3{\cdot}2HfO_2$ along with the fit values is shown in Fig. 4. The heat capacity of $Dy_2O_3{\cdot}2HfO_2$ computed by Neumann–Kopp's law using the heat capacity data of Dy_2O_3 [15] and HfO_2 [16] are also shown in Fig. 4. The heat capacity data of component oxides used for the computation are given below

$$C_{p,m}(Dy_2O_3)\left(J\ mol^{-}\ K^{-1}\right) = 124.809 + 11.59 \times 10^{-3}(T/K) - 1.607 \times 10^{6}(K/T)^2 \quad (8)$$

$$C_{p,m}(HfO_2)\left(J\ mol^{-1}\ K^{-1}\right) = 72.111 + 9.050 \times 10^{-3}(T/K) - 1.293 \times 10^{6}(K/T)^2 \quad (9)$$

As can be seen in the figure, the heat capacity data of $Dy_2O_3{\cdot}2HfO_2$ are about 2–4% less than that computed using Neumann–Kopp's law using the heat capacity of their component oxides. From the heat capacity data, other thermodynamic functions such as enthalpy, entropy and Gibbs energy functions of $Dy_2O_3{\cdot}2HfO_2$ were computed and are given in Table 2. The S^0_{298} values of $Dy_2O_3{\cdot}2HfO_2$ required for the computation of entropies are estimated by using Neumann–Kopp's law from the literature data [15, 16] of their respective component oxides is 268.61 J K^{-1} mol^{-1}, respectively, besides including the contribution of entropy of mixing.

Discussion

The percentage linear thermal expansion obtained for dysprosium hafnate computed are shown in Fig. 3 To the best of our knowledge, HT-XRD based lattice thermal expansion data for dysprosium hafnate is not available in the open literature. The room temperature lattice parameter value estimated in this study is 0.5182 nm. From Fig. 2, it is observed that the lattice parameter increases progressively with increasing temperature. The percentage linear thermal expansion also increases steadily with increasing temperature (Fig. 3). The mean linear thermal expansion coefficient for dysprosium hafnate between 298 to 2,000 K is found to be 14.89 × 10^{-6} K^{-1}.

Table 2 Thermodynamic functions of $Dy_2O_3{\cdot}2HfO_2$ solid solution

T/K	$C_{p,m}$/J K^{-1} mol^{-1})		$H^0_T - H^0_{298}$/(J mol^{-1})	S^0_T/(J mol^{-1} K^{-1})	$G^0_T - H^0_{298}/T$/(J mol^{-1} K^{-1})
	Measured	Fit			
298	232	233	0	274	−274
300	232	233	466	275	−274
400	247	245	24,317	344	−283
500	256	258	49,495	400	−301
600	269	270	75,946	448	−322
700	277	278	103,395	491	−343
800	281	283	131,487	528	−364

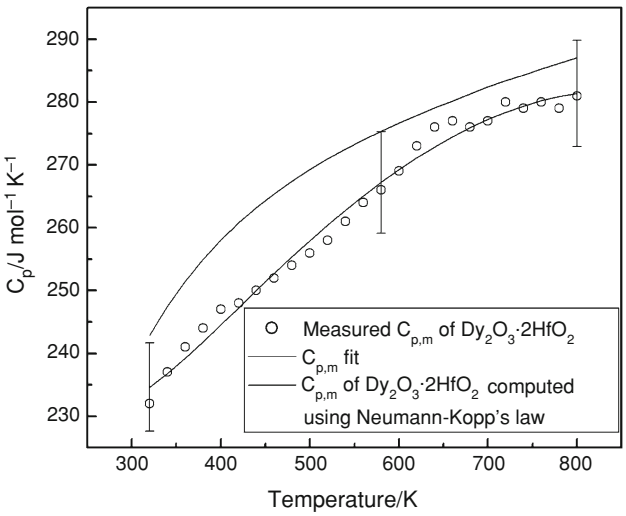

Fig. 4 Heat capacity data of Dy_2O_3·2HfO_2

The linear thermal expansion coefficient of dysprosium hafnate has been measured by Risovany et al. [5] up to 773 K. The average linear thermal expansion coefficient obtained in this study in the same temperature range is 10.5×10^{-6} K^{-1} which is slightly lower than the value reported by Risovany et al. [6] is 11.1×10^{-6} K^{-1} to 11.6×10^{-6} K^{-1} for Dy_2O_3-HfO_2 system containing 23–75 mol% HfO_2 along with 2% Nb_2O_5 in each case [6]. The different may be due to the fact that the compositions used in our study and that of Risovany et al. are different and also that HTXRD was used in the present measurement where as Risovany et al. measured the bulk thermal expansion.

Risovany et al. [6] mentioned that the heat capacity value of dysprosium hafnate is practically constant from 298 to 673 K. But our measurements show that the heat capacity increase from 233 to 275 J K^{-1} mol^{-1} in the same temperature range. This may be due to the fact that the heat capacities data of Risovany et al. [6] show large scatter and the error of the measurement is as high as 6%. The accuracy of the measured heat capacity data in the present measurement is ±3% and also the scatter in the data is less than 0.5%.

Conclusions

Heat capacity and thermal expansion measurements were carried out by DSC and HTXRD in the temperature range 298–800 K and 298–1973 K, respectively. The heat capacity and the thermal expansion characteristics of Dy_2O_3·2HfO_2 did not vary with the preparation methods. The measured heat capacity values of Dy_2O_3·2HfO_2 are 2–4% less than that computed by Neumann–Kopp's additive rule. The present data on the heat capacity of Dy_2O_3-HfO_2 solid solution is more reliable than that measured by Risovany et al. [6] due to lower scatter of the present data than that of Risovany et al. [6].

References

1. Colin M. Materianx absorbants neutroniques pour le pilotage des reacteurs nucleaires, Techniques de l'lngenieur. Genie nucleaires. 1989;B8-2:3720–5.
2. Syamala KV, Panneerselvam G, Subramanian GGS, Antony MP. Synthesis, characterization and thermal expansion studies on europium titanate. Thermochim Acta. 2008;475:76–9.
3. Panneerselvam G, Venkata Krishnan R, Antony MP, Nagarajan K, Vasudevan T, Vasudeva Rao PR. Thermophysical measurements on dysprosium and gadolinium titanates. J Nucl Mater. 2004;327(2–3):220–5.
4. Risovany VD, Varlashova EE, Suslov DN. Dysprosium titanate as an absorber materials for control rods. J Nucl Mater. 2000; 281:84–9.
5. Perova EB, Spiridonov LN, Komisarova LN. Phase equilibria in the system HfO_2 – Dy_2O_3. Inorg Mater. 1972;8:1878–80.
6. Risovany VD, Zakharov AV, Muraleva EM, Kosenkov VM, Latypov RN. Dysprosium hafnate as an absorbing material for control rods. J Nucl Mater. 2006;355:163–70.
7. DRSprink, JHSchemel. The development of rare earth pyrohafnates for power reactor control-rod materials. J Nucl Mater 1973/74;49:1–9.
8. Xue B, Li XF, Wang JY, Yu SJ, Tan ZC, Sun LX. Heat capacities and thermodynamic properties of trans-(R)-3-(2,2-dichloroethenyl)-2,2-dimethylcyclopropanecarboxylic acid. J Therm Anal Calorim. 2008;94:529–34.
9. Qiu SJ, Chu HL, Zhang J, Qi YN, Sun LX, Xu F. Heat capacities and thermodynamic properties of CoPc and CoTMPP. J Therm Anal Calorim. 2008;91:841–8.
10. Panneerselvam G, Antony MP, Vasudevan T. Studies on lattice thermal expansion and XPS of ThO_2-$NdO_{1.5}$ solid solutions. Thermochim Acta. 2006;443:109–15.
11. Venkata Krishnan R, Nagarajan K. Heat capacity measurements on uranium-cerium mixed oxides by differential scanning calorimetry. Thermochim Acta. 2006;440:141–5.
12. Powder diffraction files (Inorganic Phases), Joint Committee on Powder Diffraction Data (JCPDS), International Centre for Diffraction Data (1999). ICDD card number: 24-0360.
13. Cullity BD. Elements of X-ray diffraction, Chapter 11. 2nd ed. Reading, MA: Addison Weseley Publishing Co.; 1978.
14. Venkata Krishnan R, Nagarajan K, Vasudeva Rao PR. Heat capacity measurements on $BaThO_3$ and $BaCeO_3$. J Nucl Mater. 2001;299:28–31.
15. Spencer PJ. Thermochemical properties. In: Komarek KL, editor. Hafnium: physico-chemical properties of its compounds and alloys, Atomic Energy Reviews, vol. 8. Vienna: International Atomic Energy Agency; 1981, p. 424–7.
16. Pankratz LB. Thermodynamic properties of elements and oxides, Bull US Bur Mines. 1982.